Environmental Science & Technology

pubs.acs.org/est

Article

Biomagnification of Methylmercury in a Marine Plankton Ecosystem

Peipei Wu, Emily J. Zakem, Stephanie Dutkiewicz, and Yanxu Zhang*

Cite This: *Environ. Sci. Technol.* 2020, 54, 5446−5455

Read Online

ACCESS | Metrics & More | Article Recommendations | Supporting Information

ABSTRACT: Methylmercury is greatly bioconcentrated and biomagnified in marine plankton ecosystems, and these communities form the basis of marine food webs. Therefore, the evaluation of the potential exposure of methylmercury to higher trophic levels, including humans, requires a better understanding of its distribution in the ocean and the factors that control its biomagnification. In this study, a coupled physical/ecological model is used to simulate the trophic transfer of monomethylmercury (MMHg) in a marine plankton ecosystem. The model includes phytoplankton, a microbial community, herbivorous zooplankton (HZ), and carnivorous zooplankton (CZ). The model captures both shorter food chains in oligotrophic regions, with small HZ feeding on small phytoplankton, and longer chains in higher nutrient conditions, with larger HZ feeding on larger phytoplankton and larger CZ feeding on larger HZ. In the model, trophic dilution occurs in the food webs that involve small zooplankton, as the grazing fluxes of small zooplankton are insufficient to accumulate more MMHg in themselves than in their prey. The model suggests that biomagnification is more prominent in large zooplankton and that the microbial community plays an important role in the trophic transfer of MMHg. Sensitivity analyses show that with increasing body size, the sensitivity of the trophic magnification ratio to grazing, mortality rates, and food assimilation efficiency (AE_C) increases, while the sensitivity to excretion rates decreases. More predation or a longer zooplankton lifespan may lead to more prominent biomagnification, especially for large species. Because lower AE_C results in more predation, modeled ratios of MMHg concentrations between large plankton are doubled or even tripled when the AE_C decreases from 50% to 10%. This suggests that the biomagnification of large zooplankton is particularly sensitive to food assimilation efficiency.

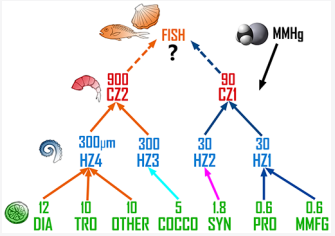

INTRODUCTION

Methylmercury (MeHg), particularly monomethylmercury (MMHg), is a potent neurotoxin that is associated with cardiovascular effects in adults and causes neurocognitive deficits in fetuses.[1−3] Globally, the consumption of marine fish and shellfish is still rising and remains the primary source of human MMHg exposure.[4−6] As the base of marine food webs, phytoplankton introduce MMHg into the food web and transmit them to higher trophic levels.[7,8] Many studies have shown that the MMHg concentrations in phytoplankton can reach 10^5 times higher than those in seawater, and concentrations in zooplankton can reach 10^5−10^6 times.[7,9] This study focuses on the biomagnification of MMHg in marine plankton food webs.

MMHg is bound to proteins and is further bioaccumulated in marine food webs.[10] Organisms at higher trophic levels have higher energy requirements and tend to eat more, which facilitates the trophic transfer of MMHg.[11] MMHg also accumulates further up the food web at higher concentrations because the lifespan of these organisms are longer.[12] Many laboratory and field studies have observed MMHg biomagnification between phytoplankton and zooplankton.[12−15] For example, Hammerschmidt et al.[12] found that in the Northwest Atlantic Ocean, the MMHg concentration in large zooplankton (1.04 ± 0.80 ng/g wet weight) was significantly higher than that in small zooplankton (0.28 ± 0.24 ng/g) due to the longer lifespan of large zooplankton.

The global plankton ecosystem has tremendous diversity with large regional differences caused by different physiological and environmental factors.[16−19] This variability influences the transmission processes of MMHg in food webs. For instance, a different marine plankton community structure will alter the bioconcentration and grazing fluxes of MMHg.[20] Dissolved organic carbon (DOC) also influences the transmission: when DOC concentrations are low, MMHg has higher bioavailability and passes through cell membranes more easily.[9]

Models have been developed to study the biomagnification of MMHg in marine food webs. The Ecotracer and Ecopath models have been applied to simulate MMHg trophic transfer in marine food webs.[21−24] However, these studies often focus on a single site, and many of the MMHg transfer processes are not connected to plankton physiological parameters. Zhang et al.[25] first linked MMHg transfer with a plankton ecosystem model (DARWIN), but it only included two trophic levels (producers and primary consumers). In contrast, Schartup et al.[9] considered a longer food chain, but it was limited to coastal, shelf, and pelagic regions of the Northwest Atlantic Ocean.

Received: October 9, 2019
Revised: February 12, 2020
Accepted: February 13, 2020
Published: February 13, 2020

https://dx.doi.org/10.1021/acs.est.9b06075
Environ. Sci. Technol. 2020, 54, 5446−5455

In this study, a coupled physical/ecosystem model is used to simulate the MMHg trophic transfer in the global marine plankton ecosystem. The MMHg transfer processes are related to an existing ecosystem model[26] that has physiological descriptions of metabolically diverse plankton, including primary producers (phytoplankton), primary consumers (herbivorous zooplankton, HZ), and a diverse microbial community including heterotrophs and chemoautotrophs (here referred to as microbial metabolic functional groups, MMFG). In addition, we extend the ecosystem model to include secondary consumers (carnivorous zooplankton, CZ) and their MMHg transfer processes. The regional variability of MMHg trophic transfer in the different trophic levels is also explored. Modeling experiments are then conducted to explore the sensitivity of MMHg biomagnification to plankton physiological parameters.

METHODS

General Description. We simulate the MMHg bioconcentration and biomagnification in the MITgcm physical framework.[27] The ocean circulation data is from the Integrated Global Systems Model (IGSM).[28] The physical model has a resolution of 2° × 2.5° horizontally with 22 vertical levels. The ocean boundary layer physics is modeled based on Large et al.,[29] and the effects of mesoscale eddies are parametrized following Gent and McWilliams.[30]

Ecosystem Model. The ocean plankton ecology and biogeochemistry are simulated by a recent ecosystem model that resolves diverse functional types as populations (schematically shown in Figure 1).[26] Briefly, the model simulates six

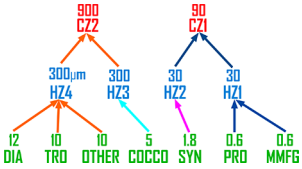

Figure 1. Schematic of modeled marine plankton food webs. The numbers above the plankton type name are the cell/body sizes in the unit of μm. The arrows connect the prey to its predator. There are six phytoplankton types: DIA (diatoms), TRO (diazotrophs), OTHER (other large phytoplankton), COCCO (coccolithophores), SYN (*Synechococcus*), PRO (*Prochlorococcus*), six MMFG (microbial metabolic functional groups), represented here though as one category as they are all the same size; four herbivorous zooplankton: HZ1, HZ2, HZ3, and HZ4; and two carnivorous zooplankton: CZ1 and CZ2.

representative categories of phytoplankton with different sizes, growth rates, affinity to nutrients and other physiological parameters. There are two small phytoplankton: *Prochlorococcus* (which do not use NO_3^- and have the lowest equilibrium resource concentrations[31]), and *Synechococcus* (which also have low equilibrium resource concentrations); three large phytoplankton groups: diatoms (with hard silica shells and using silica), diazotrophs (which fix nitrogen), and other large eukaryotic phytoplankton; and intermediately sized coccolithophores (with calcium carbonate plates). Six microbial metabolic functional groups (MMFG) are also included: aerobic heterotrophic bacteria that consume dissolved organic matter (DOM) and sinking particulate organic matter (POM), anaerobic nitrate-reducing ($NO_3^- \rightarrow NO_2^-$), anaerobic denitrifying ($NO_2^- \rightarrow N_2$), anaerobic NH_4^+ oxidizing (anammox, $NH_4^+ \rightarrow N_2$), NH_4^+ oxidizing ($NH_4^+ \rightarrow NO_2^-$), and NO_2^- oxidizing ($NO_2^- \rightarrow NO_3^-$) microorganisms. In the remainder of this article, we will consider the six microbial groups as a single entity (i.e., MMFG) as they are modeled as the same size, and our study focuses on the trophic interactions which are set as a function of size. Remineralization of organic matter proceeds as a function of organic matter consumption and respiration by the heterotrophic groups. Labile dissolved and particulate organic matter are explicitly modeled and sourced from the mortalities of all populations,[26] while recalcitrant DOC is an input into the model from an established data set.[32] The total (recalcitrant and labile) DOC impacts microbial and phytoplankton MMHg content according to eq 1 below, while only the labile DOC affects microbial growth. Four HZ types graze on phytoplankton and MMFG in size classes: HZ1 grazes on *Prochlorococcus* and the six MMFG, HZ2 on *Synechococcus*, HZ3 on coccolithophores, and HZ4 on large phytoplankton groups (diatoms, diazotrophs, and other large phytoplankton).

New to this study, we add two CZ groups into the ecosystem model. The smaller one (CZ1) grazes on smaller HZ (HZ1 and HZ2), and the larger one (CZ2) grazes on larger HZ (HZ3 and HZ4) (Figure 1). Physiological parameters of CZ and HZ are a function of body size following Taniguchi et al. (Table S1).[33] We numerically integrate the ecosystem model forward in time until the biomass of each plankton reach a seasonally varying quasi-steady state (20 years). The plankton biomass, grazing fluxes, and mortality rates from this steady state serve as an input for the methylmercury model. The mortality rate represents all losses other than grazing (viral lysis, cell death) for MMFG, phytoplankton, and HZ but also includes a parametrization of loss to higher trophic levels for the CZ (as no predators for CZ are explicitly modeled).

Methylmercury Model. The methylmercury model is based on Zhang et al.[25,34] which simulates the transport and biogeochemical processes of marine methylmercury cycle, including river discharge, air-sea exchange, sinking of particle mercury, redox reactions, methylation, demethylation, and bioconcentration and biomagnification in marine plankton food webs. We also extend their model to include newly introduced MMFG and CZ species.

Phytoplankton and MMFG accumulate MMHg primarily by passive uptake from seawater (diffusion) across the cell membrane

$$\mathrm{MMHg}_{\mathrm{phy}} = \mathrm{VCF}(d, [\mathrm{DOC}])\cdot \mathrm{MMHg}_{\mathrm{sea}} \quad (1)$$

where $\mathrm{MMHg}_{\mathrm{phy}}$ and $\mathrm{MMHg}_{\mathrm{sea}}$ are the MMHg concentrations in phytoplankton/MMFG and seawater, respectively. The volume concentration factor (VCF) is a function of the cell diameter d and total DOC concentrations (Table S1).[9]

The transfer of MMHg in herbivorous and carnivorous zooplankton includes the following processes: (1) direct MMHg intake from seawater; (2) uptake of MMHg by predation; (3) MMHg released by death; (4) maternal transfer; and (5) excretion of MMHg

$$\frac{\mathrm{dMMHg}_{\mathrm{pred}}}{\mathrm{dt}} = k_{\mathrm{BC}}\cdot \mathrm{MMHg}_{\mathrm{sea}} - (k_{\mathrm{MT}} + k_{\mathrm{MA}} + k_{\mathrm{EX}})\cdot \mathrm{MMHg}_{\mathrm{pred}} + k_{\mathrm{GR}}\cdot \mathrm{AE}_{\mathrm{MMHg}}\cdot \mathrm{MMHg}_{\mathrm{prey}} \quad (2)$$

where $\mathrm{MMHg}_{\mathrm{pred}}$ is the MMHg concentrations in predators (i.e., HZ or CZ), $\mathrm{MMHg}_{\mathrm{prey}}$ is the MMHg concentrations in

https://dx.doi.org/10.1021/acs.est.9b06075
Environ. Sci. Technol. 2020, 54, 5446−5455

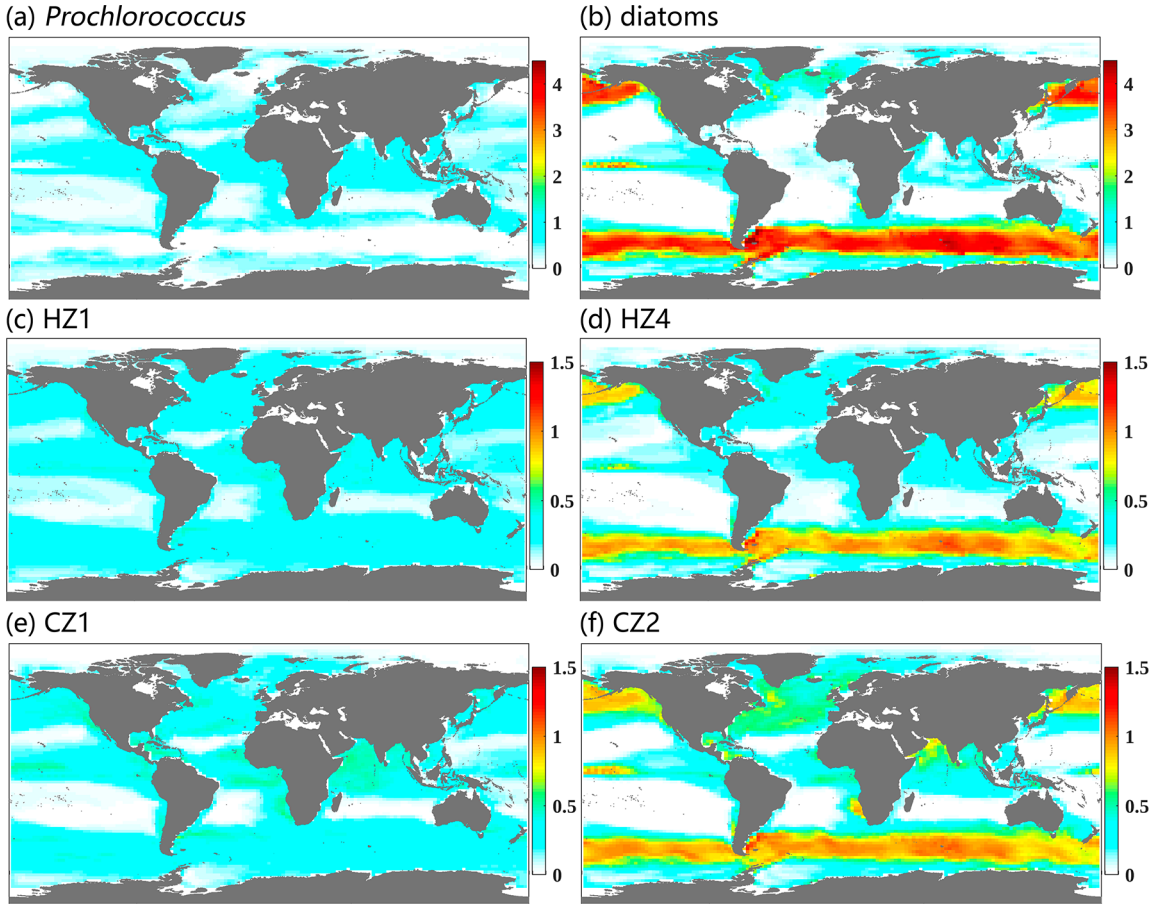

Figure 2. Modeled spatial distributions of the selected plankton biomass in the global euphotic zone [mmol C m^{-3}]. (a) *Prochlorococcus*; (b) diatoms; (c) small herbivorous zooplankton HZ1; (d) large herbivorous zooplankton HZ4; (e) small carnivorous zooplankton CZ1; and (f) large carnivorous zooplankton CZ2.

prey (i.e., phytoplankton, MMFG or HZ), and $MMHg_{sea}$ is the MMHg concentrations in seawater. AE_{MMHg}, k_{BC}, k_{MT}, k_{MA}, k_{EX}, and k_{GR} are the MMHg assimilation efficiency, bioconcentration rate, mortality rate, maternal transfer rate, excretion rate, and grazing rate for the predator, respectively (Table S1).

The rate parameters are related to the volume and mass of plankton bodies as well as environmental parameters such as seawater temperature.[35] The AE_{MMHg} for HZ and CZ range from 50%−70% and 75%−95% respectively,[9] and 60% and 90%, respectively, are chosen in this study. More details of the model are available in the Supporting Information. The model is run from 2000 to 2015 with the initial condition from Zhang et al.,[25] and we use the results of the last year for the following analyses. The atmospheric mercury concentration and deposition fluxes are taken from the output of GEOS-Chem model.[36]

Sensitivity Analysis. The trophic transfer of MMHg relies on plankton food web dynamics, such as grazing, excretion, maternal transfer, mortality, and the assimilation efficiency of carbon (AE_C, i.e. food assimilation efficiency). To save computational costs, a box model is used instead of a 3-D simulation to test the sensitivity of the physiological rates. In the box model, the concentrations of MMHg and the parameters of the plankton ecosystem are taken as the global means in the euphotic zone of the 3-D methylmercury and ecosystem models, respectively. In the box model, the grazing, mortality, and excretion rates are varied from 0.1 to 10 times the original values used in the 3-D model. The AE_C is varied from 10% to 100% in the 3-D ecosystem simulation. The changes of MMHg concentrations in all possible model food chains are calculated as an indicator of biomagnification.

RESULTS AND DISCUSSION

Ecosystem Model. We analyze the results of the modeled euphotic zone (the top 115 m) where most (75%) of the phytoplankton and zooplankton are sustained. Figure 2 shows the spatial distributions of the biomass of selected plankton functional groups (results for the other groups are available in Figure S1). Overall, the modeled distributions of phytoplankton and HZ are consistent with the previous model results[16,37] and observations.[38,39] As observed, small phytoplankton functional groups (*Prochlorococcus* and *Synechococcus*) are more ubiquitous and dominate in the oligotrophic oceans (e.g., subtropical oceans) while the large groups (diatoms and the other large phytoplankton) bloom in the eutrophic areas (e.g., regions of upwelling: high-latitude oceans, such as the Southern Ocean and the equatorial regions).[40,41] Like total phytoplankton and zooplankton, MMFG have higher biomass in the eutrophic regions where production rates are higher (Figure S2c).[42] As source of food, the spatial distributions of phytoplankton restrict those of HZ (Figure 2c,d), which further restrict those of CZ (Figure 2e,f).[43]

The spatial distributions of phytoplankton groups are similar to previous modeling results without CZ, indicating that the

https://dx.doi.org/10.1021/acs.est.9b06075
Environ. Sci. Technol. 2020, 54, 5446−5455

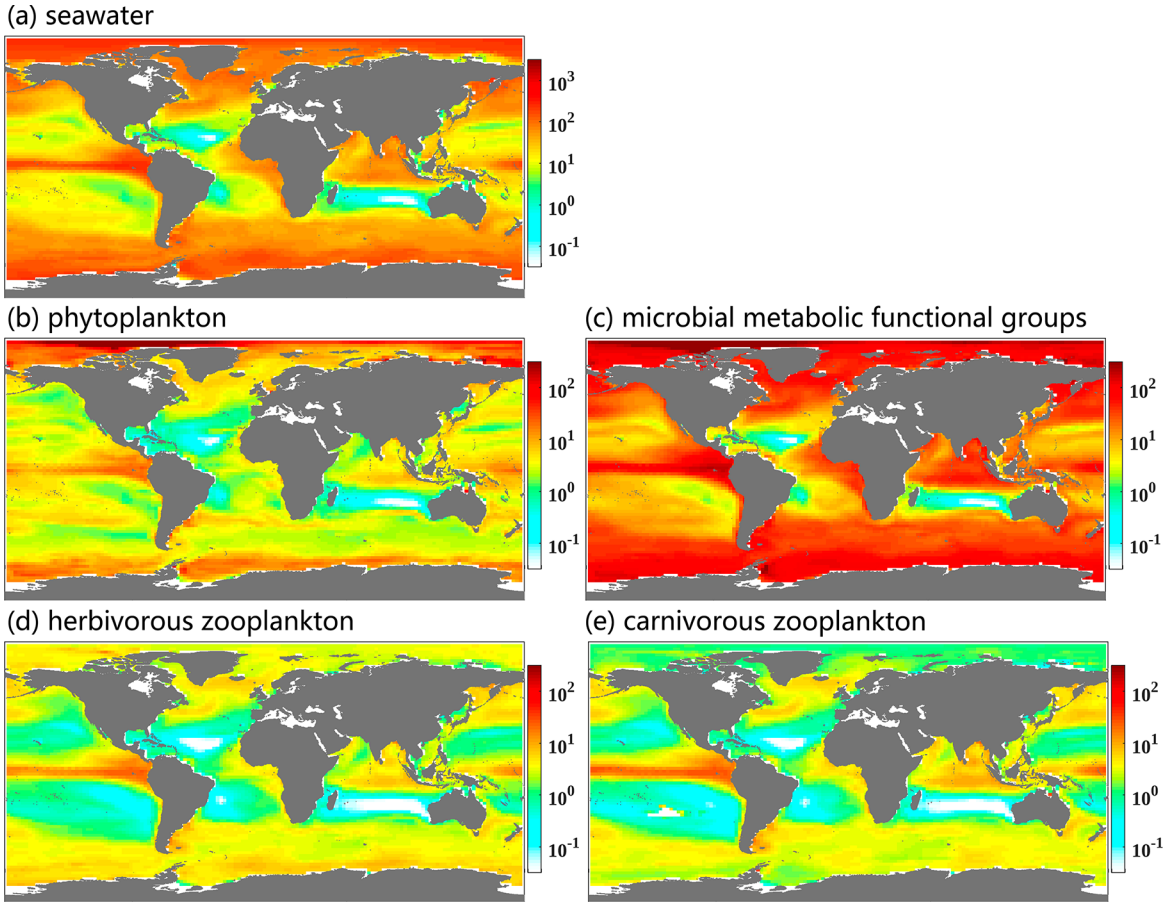

Figure 3. Modeled spatial distributions of the MMHg concentrations in the seawater [fM] (1fM = 10^{-15} mol/L) and different plankton functional groups (ng/g wet weight) in the global euphotic zone. (a) Seawater [fM]; (b) phytoplankton; (c) microbial metabolic functional groups; (d) herbivorous zooplankton; and (e) carnivorous zooplankton.

locations where the different types dominate are not significantly affected by the inclusion of predators two trophic level higher.[44] However, the addition of CZ increases the global total biomass of phytoplankton groups by 158% compared to the simulation without CZ, and decreases that of HZ by 22%. This is because the inclusion of CZ increases predation pressure on HZ, which is unfavorable for their accumulation of biomass, and this in turn benefits phytoplankton and increases their biomass.[45] The modeled total primary production (PP) of global oceans is 53 Pg/year, which is within the estimate of 44−67 Pg/year based on satellite data.[46]

Methylmercury Model. Figure 3a shows the spatial distribution of MMHg in the model surface ocean. Relatively high MMHg concentrations are simulated in the high latitude oceans and the equatorial Pacific Ocean, while there are low concentrations in the mid- and low-latitude oceans. This pattern reflects the influence of solar radiation and temperature.[25] Figure 2b−e maps the MMHg concentrations in the different groups of plankton (phytoplankton, MMFG, HZ, and CZ). Figure 4 illustrates the trophic transfer fluxes of MMHg between individual types.

MMHg in Phytoplankton and MMFG. High MMHg concentrations in phytoplankton are modeled in the high-latitudes and the eastern equatorial Pacific oceans, due to both high plankton biomass and high MMHg concentrations in the seawater (Figure 2a,b, Figure 3b,c). Small phytoplankton species, such as *Prochlorococcus* and *Synechococcus*, have large cell surface area to volume ratios and subsequently high MMHg uptake efficiencies, contributing to the relatively high concentrations in tropical regions.[47] This is consistent with the modeled results by Zhang et al.[25] The spatial pattern of MMHg concentrations in MMFG is similar to that of phytoplankton, and the concentrations are at least twice as large as those in phytoplankton due to their even smaller sizes and hence even larger surface to volume ratios (Figures 3c and 4).

The concentrations of MMHg in this study are reported as a wet weight, unless otherwise noted. The modeled global average MMHg concentrations in the large phytoplankton range between 0.7 and 3.6 ng/g wet weight, which is consistent with measurements in the central Pacific (0.1−4 ng/g).[48] The modeled MMHg concentrations in the small phytoplankton and MMFG are much higher (8.3−35.3 ng/g). Unfortunately, there are no observations of concentrations in these small size classes to evaluate the model. However, higher concentrations in smaller classes have been hypothesized given their higher surface to volume ratios.[49] As the MMFG have high concentrations of MMHg, this leads to a high trophic transfer to their predators, HZ1. Indeed, this model predicts 2204 kmol/yr of MMHg transferred by MMFG to herbivorous zooplankton, which is larger than the transfer from any other type of the phytoplankton groups to the zooplankton (Figure 4).

MMHg in Zooplankton. MMHg in zooplankton comes from both seawater and food. In this model, the contribution

https://dx.doi.org/10.1021/acs.est.9b06075
Environ. Sci. Technol. 2020, 54, 5446−5455

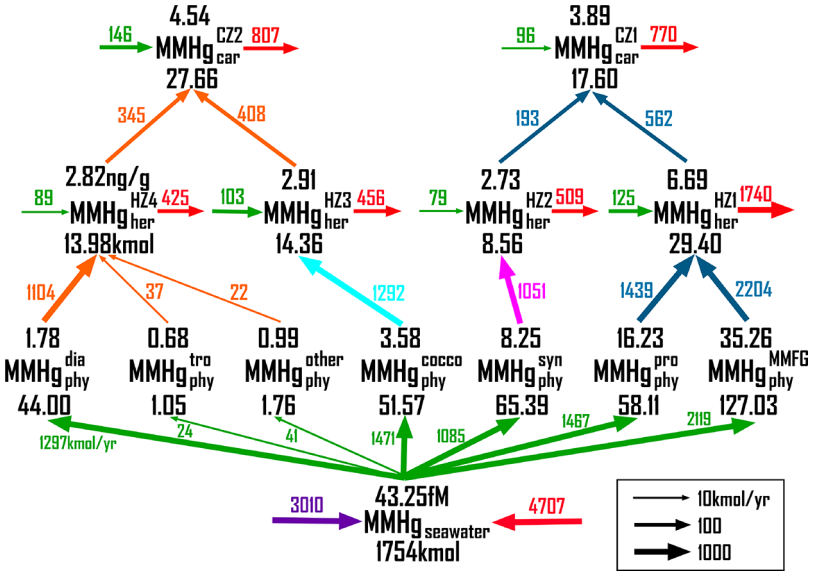

Figure 4. Trophic transfer of MMHg in global plankton food webs. The numbers above the seawater and the planktons are the MMHg concentrations in units of fM (1 fM = 10^{-15} mol/L) and ng/g wet weight, respectively, and those below are the total mass of MMHg in units of kmol. The green arrows are for the bioaccumulation fluxes from seawater to plankton. The red arrows are for the release of MMHg from zooplankton by death, excretion, and maternal transfer. The purple arrow pointing to the bottom MMHg symbol represents the sloppy grazing flux. The other colors are for the grazing fluxes of MMHg by zooplankton. The width of these arrows are proportional to the logarithm of the magnitudes of the fluxes. The plankton groups include six types of primary producers: dia (diatoms), tro (diazotrophs), large (other large phytoplankton), cocco (coccolithophores), syn (*Synechococcus*), and pro (*Prochlorococcus*); MMFG (microbial metabolic functional groups, the six types are grouped together here as they are all the same size); the four herbivorous zooplankton (her): HZ1, HZ2, HZ3, and HZ4; and two carnivorous zooplankton (car): CZ1 and CZ2.

of MMHg directly obtained from seawater is small (7%), and grazing is the primary cause of MMHg biomagnification (Figure 4).[9,50] The spatial patterns of the MMHg concentrations in the different zooplankton are similar, with higher MMHg concentrations in the productive equatorial and high-latitude oceans and lower concentrations in the oligotrophic subtropical oceans (Figure 3d,e). The spatial pattern of the MMHg concentrations in HZ is consistent with Schartup et al.[9] However, they simulated lower MMHg concentrations in omnivorous zooplankton due to "growth dilution" in productive areas where nutrients were abundant. Here, "growth dilution" refers to the increase in biomass that exceeds the accumulation of MMHg, resulting in a decrease in MMHg concentration per body weight. The differences between our model results and those of Schartup et al. arise from the parametrization of zooplankton grazing and growth.[9] Modeled average MMHg concentrations in zooplankton range from 2.7 to 6.7 ng/g, which overlap with the range of 0.2−3.4 ng/g observed in the central Pacific[48] and 1.9−4.1 ng/g in the Southern Ocean.[51]

The modeled MMHg concentrations in large HZ (HZ3 and HZ4) are slightly higher than those in small ones (HZ2). A similar trend with size is modeled for CZ, with higher MMHg concentrations in the larger CZ2 compared to the smaller CZ1. This is consistent with empirical studies that have observed higher MMHg concentrations in large size bins of zooplankton samples in several aquatic environments (Northwest Atlantic Ocean, central Pacific Ocean, Onondaga Lake and Lake Lusignan).[12,48,52,53] One exception here is HZ1, which has the highest MMHg concentrations due to the contribution from MMFG (Figure 4). Kainz and Mazumder[50] found that, although bacteria (included in MMFG) were less nutritious and comprised a smaller portion of the HZ diet, the HZ MMHg concentrations were strongly affected by those found in the MMFG. In their study, bacteria could predict 50% of the variation of MMHg concentrations in the food web. This confirms our finding that the microbial community plays an important role in the trophic transfer of MMHg (Figure 4). In addition, anaerobic bacteria may stay alive in the intestinal tracts of zooplankton and produce MMHg.[54] However, MMHg in the microbial community is still poorly understood, and MMHg trophic transfer from this group to higher trophic levels is often neglected. More studies of MMHg accumulation and trophic transfer of the microbial community are thus needed. Our study suggests this route of bioaccumulation may be important.

In general, modeled MMHg concentrations in zooplankton are low where total DOC concentrations are high. For example, the average modeled zooplankton MMHg concentrations are 1.4 ng/g in low latitude oceans (except the tropical oceans), where DOC concentrations are generally higher than 60 μM (Figure 3d,e, Figure S2b). This agrees with Schartup et al.,[9] who found that MMHg concentrations in zooplankton decreased with increasing DOC concentrations. In our simulation, DOC concentrations increase in oligotrophic areas because of the imposed nonreactive, "recalcitrant" DOC (Figure S2b). In contrast, the concentrations of "labile" DOC that fuel microbial growth are low where these recalcitrant DOC concentrations are high (Figure S2a). Observations have showed similar trends: the zooplankton MMHg concentrations in the Southern Ocean (1.9−4.1 ng/g)[51] were higher than in the tropical coastal Pacific Ocean (0.69−3 ng/g),[55] where the DOC concentrations were approximately 30 μM higher. Higher concentrations of DOC lead to less MMHg entering phytoplankton, which in turn results in less MMHg uptake by zooplankton. One difference

https://dx.doi.org/10.1021/acs.est.9b06075
Environ. Sci. Technol. 2020, 54, 5446−5455

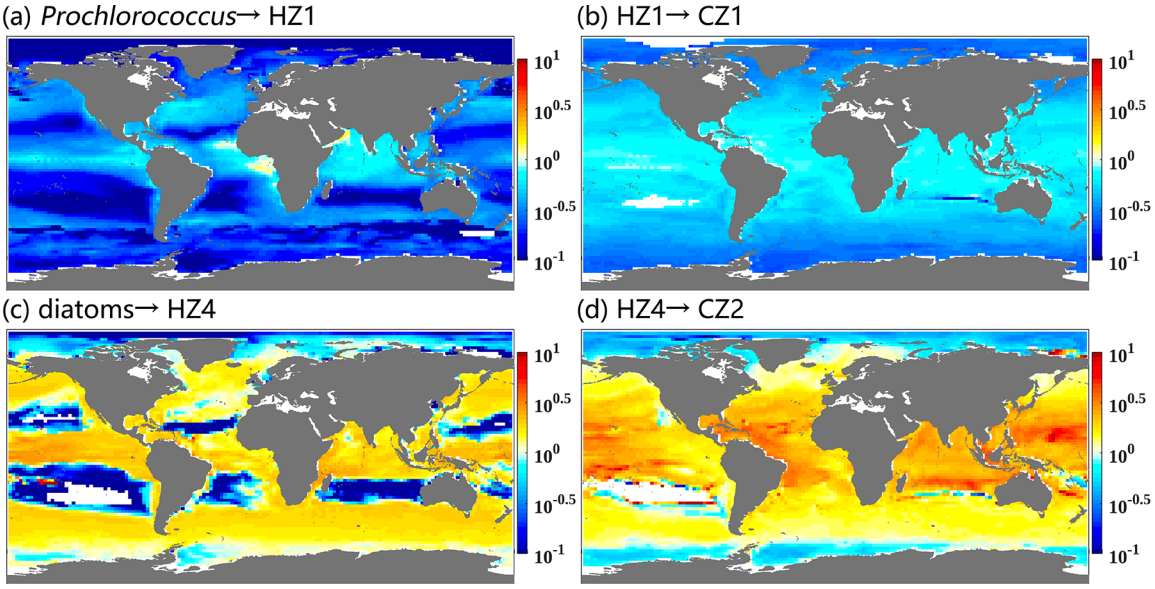

Figure 5. Modeled ratios of MMHg concentrations per wet plankton biomass between two consecutive trophic levels (TMRs) in the global ocean: (a) between small herbivorous zooplankton HZ1 and *Prochlorococcus*; (b) between small carnivorous zooplankton CZ1 and HZ1; (c) between large herbivorous zooplankton HZ4 and diatoms; and (d) between large carnivorous zooplankton CZ2 and HZ4. No value indicates that one or both of the plankton are not present in that location.

between the results of our model and those of Schartup et al. is that our model predicts relatively high MMHg concentrations in zooplankton in the equatorial oceans where DOC concentrations are high, which is consistent with the observations in the central Pacific Ocean.[48] In this model, the high MMHg concentrations are a result of *in situ* production and upwelling from subsurface water.[25] In contrast, Schartup et al.[9] assumed that the MMHg concentration in seawater was constant (50 fM). This indicates that the DOC and MMHg in seawater and phytoplankton both influence the MMHg concentrations in zooplankton.[8,9]

MMHg Biomagnification. The MMHg magnification ratio between two trophic levels is defined as the trophic magnification ratio (TMR) in this study

$$\mathrm{TMR} = \frac{\mathrm{MMHg_j}}{\mathrm{MMHg_i}} \quad (3)$$

where i and j are the trophic levels (j > i), and $\mathrm{MMHg_j}$ and $\mathrm{MMHg_i}$ are the MMHg concentrations in plankton at trophic level j and trophic level i, respectively.

Figure 5 shows the modeled TMR values for two representative food chains: *Prochlorococcus* → HZ1→ CZ1 (which starts from a small phytoplankton) and diatoms → HZ4 → CZ2 (which starts from a large phytoplankton). The TMRs for other possible model food chains are available in Figure S3. The TMRs of HZ1/*Prochlorococcus* and CZ1/HZ1 are both less than one, which indicates trophic dilution in this food chain. The low grazing flux (a result of low biomass of the prey) and the assimilation efficiency of MMHg result in the small predators not accumulating more MMHg in themselves than in their prey. In addition, the elimination rates of MMHg for small zooplankton are higher than for large zooplankton (Figure 4), which is unfavorable for the bioaccumulation of MMHg. In contrast, large zooplankton have higher food intake (more prey), which results in higher accumulated MMHg concentrations than in their prey. This leads to trophic biomagnification in this food chain.[9] The global mean TMR between CZ and HZ is 0.83 for the small food chain, and 1.8 for the large one. The other food chains (Figure S3) show similar patterns. Generally, biomagnification in large plankton food chains are more significant than in small ones. This is consistent with observations that the MMHg concentrations in all but the smallest zooplankton were higher than in phytoplankton in the Northwest Atlantic Ocean.[12]

In the oligotrophic regions, such as the subtropical ocean, the TMRs of HZ/phytoplankton are low (Figure 5a,c), while the TMRs of CZ/HZ are high (Figure 5b,d), in contrast to the eutrophic areas at high latitudes and the equator. Schartup et al.[9] modeled the same phenomenon in the Northwest Atlantic Ocean. In the oligotrophic oceans, due to insufficient nutrients, phytoplankton grow slowly and are subject to less grazing stress by HZ.[16] For CZ, the ecosystem model simulates higher grazing fluxes per biomass here (35 and 56 mmol C $\mathrm{year^{-1}}$ for CZ1 and CZ2, respectively) than in the eutrophic oceans (19 and 22 mmol C $\mathrm{year^{-1}}$ for CZ1 and CZ2, respectively). Despite sufficient food in the eutrophic oceans, the larger food uptake fails to compensate for the reduced MMHg concentrations caused by larger biomass, in contrast to the oligotrophic oceans.[9] Thus, this mechanism explains the modeled higher TMRs of CZ/HZ for MMHg in the oligotrophic oceans.

Available empirical studies are limited for comparison of modeled MMHg TMRs due to differences in units used (e.g., dry versus wet weight basis), measurements of whole organisms vs specific tissues, and the uneven coverage of tropic levels.[20] One study[56] in the Long Island Sound found a TMR between phytoplankton and zooplankton of 2.3, while another[12] on the continental margin of the Northwest Atlantic Ocean suggested a value of 4. This model is not well suited for coastal studies due to relatively coarse resolution, but these numbers do provide a range against which we can evaluate the model. The modeled mean TMR between phytoplankton and HZ is 2.0 in the Long Island Sound and ranges from 1.8 to 6.7 on the continental margin of the Northwest Atlantic Ocean, providing some confidence in the model. The modeled mean

https://dx.doi.org/10.1021/acs.est.9b06075
Environ. Sci. Technol. 2020, 54, 5446−5455

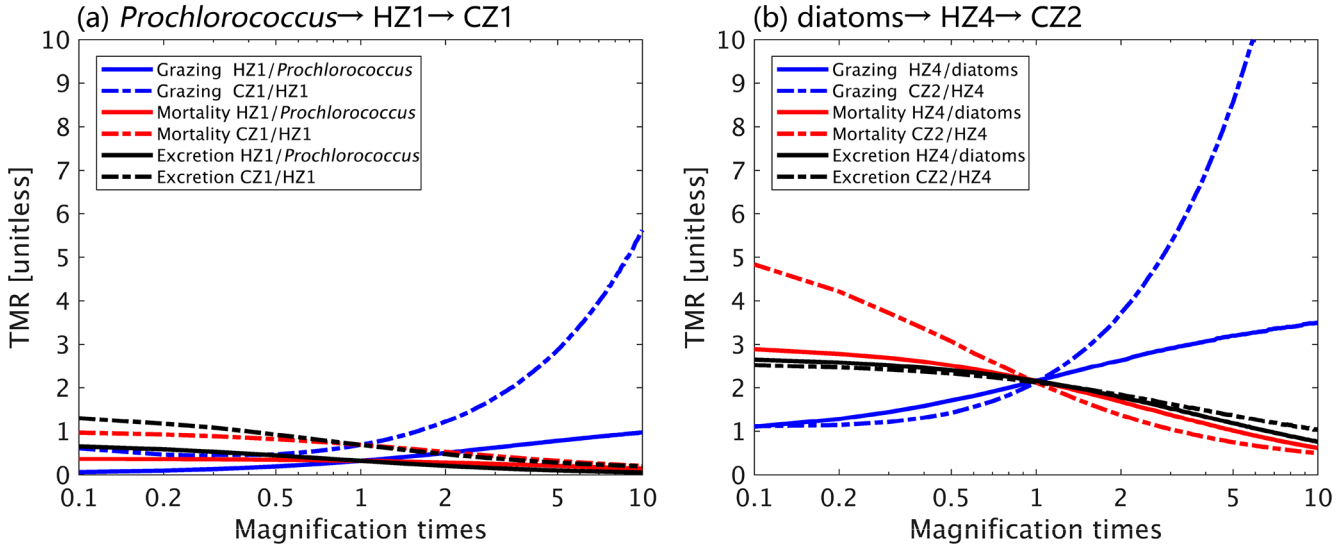

Figure 6. Effects of changing plankton physiological parameters (including grazing, mortality, and excretion rates) on the trophic magnification ratios (TMR) in the two food chains: (a) *Prochlorococcus* → small herbivorous zooplankton HZ1 → small carnivorous zooplankton CZ1; and (b) diatoms → large herbivorous zooplankton HZ4 → large carnivorous zooplankton CZ2.

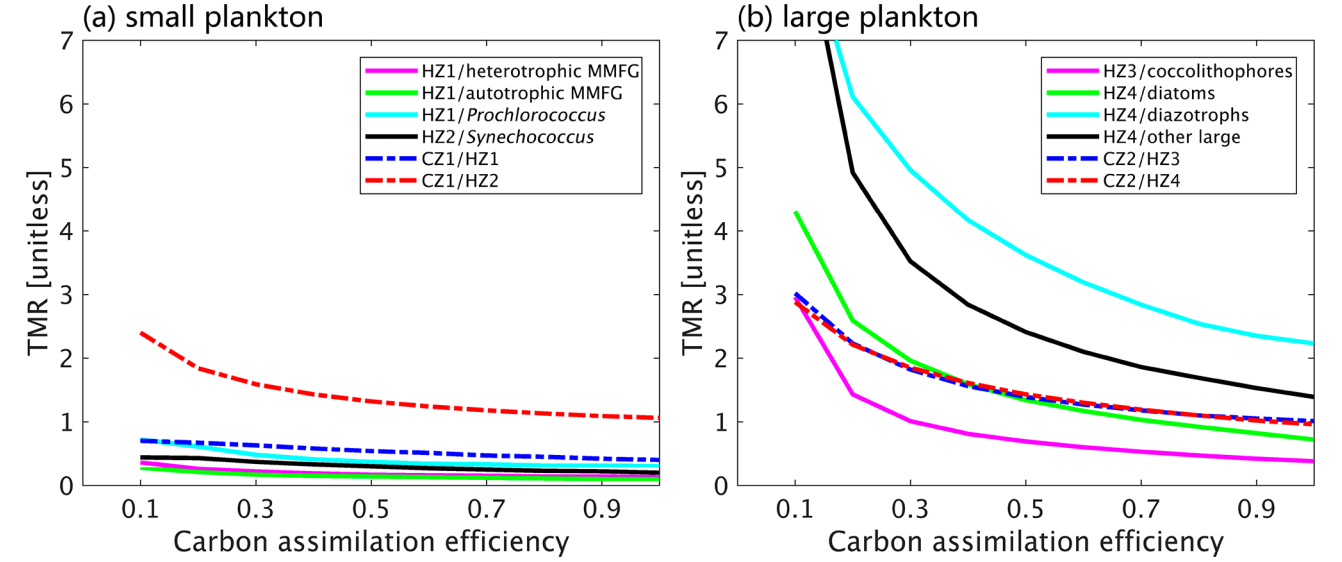

Figure 7. Effects of changing carbon assimilation efficiency (AE_C) on the trophic magnification ratios (TMR) in all possible model food chains in this study: (a) small phytoplankton (including *Prochlorococcus* and *Synechococcus*), MMFG (heterotrophic MMFG, autotrophic MMFG), small herbivorous zooplankton (HZ1 and HZ2), and small carnivorous zooplankton (CZ1); (b) large phytoplankton (including diatoms, diazotrophs, and other large phytoplankton), large herbivorous zooplankton (HZ3 and HZ4), and large carnivorous zooplankton (CZ2).

TMR between phytoplankton and HZ in the central Pacific Ocean is 1.0, which is consistent with the observed comparable MMHg concentrations of phytoplankton and zooplankton in this area.[48] The observed TMR between HZ and phytoplankton was approximately 3.0 in the northeastern Chukchi Sea,[57] 3.7 in Guanabara Bay,[58] and 0.8−9.3 in Hudson Bay[59] based on dry weight concentrations. The range of modeled TMRs for these areas is 1.0−1.4, 1.3−1.5, and 0.2−1.3 respectively. The model underestimation is due to the higher fractions of the dry weight (a function of carbon content) to wet weight of phytoplankton compared to those of zooplankton.[60,61]

Sensitivity Analyses. Figure 6 shows the sensitivity of TMRs to the physiological parameters of the two representative food chains, as above-mentioned. The results for the other food chains are shown in Figure S4. We explore the model sensitivity to the parameters describing grazing, mortality, and excretion rates (see Methods). Generally, higher grazing rates, lower mortality, and lower excretion rates increase TMRs, although the magnitudes of the changes vary with different food chains and trophic levels. The sensitivity of TMRs to grazing and mortality rates are larger in large plankton food webs than in small ones, in contrast to the sensitivity of excretion rates (Figures 6 and S4). TMRs of large zooplankton are highly sensitive to changes in grazing rates since MMHg obtained from prey is the primary source for zooplankton (Figure 6b). The TMRs are also sensitive to mortality rates, as lower mortality rates lead to longer lifetimes of MMHg in plankton bodies, which results in higher MMHg concentrations, especially for large zooplankton. The TMR of CZ2/HZ4 is increased from 2.0 to ∼10, if the grazing rate is

https://dx.doi.org/10.1021/acs.est.9b06075
Environ. Sci. Technol. 2020, 54, 5446−5455

increased by five times, and increased to ~5 if the mortality rate is decreased to 10% of the original value (Figure 6b). The sensitivity of HZ4/diatoms to these two parameters is smaller compared to the upper trophic level (Figure 6b). The influence of excretion rates on TMRs is relatively small for large zooplankton, but for small plankton, it exceeds the influence of mortality rates (Figure 6a,b).

It is found that the modeled trophic dilution is relatively robust in small plankton food chains, as the TMRs between small HZ and phytoplankton are relatively insensitive to changes in the plankton physiological rates (Figure 6a). The TMR remains less than one when the grazing rate is increased by ten times (Figure 6a, S4a−c). Similarly, 10-fold reductions in mortality and excretion rates do not cause a trophic magnification of MMHg (i.e., TMR > 1). The result indicates that in a real ocean environment, MMHg biomagnification is unlikely to happen between small HZ and phytoplankton. However, the TMRs between small CZ and HZ are sensitive to changes in grazing rates. For CZ1 and HZ1, MMHg magnification begins to occur (i.e., TMR = 1) when the grazing rate is increased 1.6 times and is prominent (TMR = 3) when the grazing rate is increased five times (Figure 6a). Changes in mortality and excretion rates do not significantly alter the TMRs between the small CZ and HZ.

Figure 7 shows the global average MMHg TMRs for all possible model food chains as a function of the carbon assimilation efficiency (AE_C). The AE_C can reach a maximum of 0.7 when the quality of the food is very high (N and Fe quotas are full)[43] but ranges between 0.2 and 0.4 for parameter values more reasonable for the real ocean.[62] The biomass and population of zooplankton both decrease when AE_C is lower, as less food is assimilated and *vice versa*.[43] Conversely, a lower AE_C increases the biomass and population of phytoplankton and MMFG due to less predation stress. Figure 7 indicates that these changes in the plankton community structure can propagate to the bioaccumulation of MMHg.

Generally, a low AE_C results in more prominent MMHg biomagnification. To get enough energy, zooplankton consume more prey when AE_C is lower, which transfers more MMHg from the prey species to predators. Under ideal conditions, the biomass of consumed prey and MMHg transfer flux are proportional to the inverse of AE_C. This is especially the case for large plankton with the TMRs increasing more rapidly when AE_C approaches zero. The TMRs are almost doubled when AE_C decreases from 50% to 10% for large CZ/HZ and are even tripled for large HZ/phytoplankton (Figure 7b). The variabilities among species are caused by the differences in mortality, excretion, and food web dynamics (Figures 4 and 6). However, TMRs for small plankton are relatively insensitive to AE_C in a range of 0.1−1, and the trophic dilution (i.e., TMR < 1) of MMHg is still modeled even for an unrealistic low AE_C value of 0.1 (except TMR between CZ1 and HZ2), probably due to their low energy requirements (Figure 7a). TMR values larger than one could be modeled if the AE_C value is further lowered, but it is of little relevance in the real ocean ecosystems.

The sensitivity analysis is conducted using a box model with parameters selected as the global averages (except AE_C, which uses 3-D models). Therefore, the sensitivity results are considered illustrative given the large spatial variability in MMHg concentrations and TMRs (Figures 3 and 5). However, the contrast between small and large plankton (i.e., Figure 6a vs 6b and Figure 7a vs 7b) indicates that the overall sensitivity of TMRs to these parameters (i.e., grazing and mortality rates, AE_C) increases with plankton body size. This suggests that MMHg may accumulate as a function of plankton size rather than species.[50] Observations of MMHg concentrations in different plankton size fractions over large spatial scale (e.g., reference 48) are thus extremely helpful for our understanding of the MMHg bioaccumulation pattern in marine food webs.

■ ASSOCIATED CONTENT

Supporting Information

The Supporting Information is available free of charge at https://pubs.acs.org/doi/10.1021/acs.est.9b06075.

Model parametrization and results (PDF)

■ AUTHOR INFORMATION

Corresponding Author

Yanxu Zhang − *Joint International Research Laboratory of Atmospheric and Earth System Sciences, School of Atmospheric Sciences, Nanjing University, Nanjing, Jiangsu 210023, China;* orcid.org/0000-0001-7770-3466; Email: zhangyx@nju.edu.cn

Authors

Peipei Wu − *Joint International Research Laboratory of Atmospheric and Earth System Sciences, School of Atmospheric Sciences, Nanjing University, Nanjing, Jiangsu 210023, China*

Emily J. Zakem − *Department of Earth, Atmospheric, and Planetary Sciences, Massachusetts Institute of Technology, Cambridge, Massachusetts 02139, United States; Department of Biological Sciences, University of Southern California, Los Angeles, California 90089, United States*

Stephanie Dutkiewicz − *Department of Earth, Atmospheric, and Planetary Sciences, Massachusetts Institute of Technology, Cambridge, Massachusetts 02139, United States*

Complete contact information is available at: https://pubs.acs.org/10.1021/acs.est.9b06075

Notes

The authors declare no competing financial interest.

■ ACKNOWLEDGMENTS

The authors gratefully acknowledge financial support from National Natural Science Foundation of China (NNSFC) 41875148, Start-up fund of the Thousand Youth Talents Plan, Jiangsu Innovative and Entrepreneurial Talents Plan, and the Collaborative Innovation Center of Climate Change, Jiangsu Province.

■ REFERENCES

(1) Budnik, L. T.; Casteleyn, L. Mercury pollution in modern times and its socio-medical consequences. *Sci. Total Environ.* **2019**, *654*, 720−734.

(2) Axelrad, D. A.; Bellinger, D. C.; Ryan, L.; Woodruff, T. J. Dose-response relationship of prenatal mercury exposure and IQ: an integrative analysis of epidemiologic data. *Environ. Health Perspect.* **2007**, *115* (4), 609−615.

(3) Sakamoto, M.; Tatsuta, N.; Izumo, K.; Phan, P. T.; Vu, L. D.; Yamamoto, M.; Nakamura, M.; Nakai, K.; Murata, K. Health impacts and biomarkers of prenatal exposure to methylmercury: lessons from Minamata, Japan. *Toxics* **2018**, *6* (3), 45.

(4) FAO *FAO Yearbook of Fishery and Aquaculture Statistics*. FAO: 2017.

(5) Sunderland, E. M.; Li, M.; Bullard, K. Decadal changes in the edible supply of seafood and methylmercury exposure in the United States. *Environ. Health Perspect.* **2018**, *126* (1), 17006−17006.
(6) Visnjevec, A. M.; Kocman, D.; Horvat, M. Human mercury exposure and effects in Europe. *Environ. Toxicol. Chem.* **2014**, *33* (6), 1259−1270.
(7) Wu, P.; Kainz, M. J.; Bravo, A. G.; Åkerblom, S.; Sonesten, L.; Bishop, K. The importance of bioconcentration into the pelagic food web base for methylmercury biomagnification: A meta-analysis. *Sci. Total Environ.* **2019**, *646*, 357−367.
(8) Pomerleau, C.; A.Stern, G.; Pućko, Monika; L.Foster, K.; W.Macdonald, R.; Fortier, Louis Pan-Arctic concentrations of mercury and stable isotope ratios of carbon (δ13C) and nitrogen (δ15N) in marine zooplankton. *Sci. Total Environ.* **2016**, *551* (1), 92−100.
(9) Schartup, A. T.; Qureshi, A.; Dassuncao, C.; Thackray, C. P.; Harding, G. C.; Sunderland, E. M. A model for methylmercury uptake and trophic transfer by marine plankton. *Environ. Sci. Technol.* **2018**, *52* (2), 654−662.
(10) Mergler, D.; Anderson, H. A.; Chan, L. H. M.; Mahaffey, K. R.; Murra, M.; Sakamoto, M.; Stern, A. H. Methylmercury exposure and health effects in humans: a worldwide concern. *Ambio* **2007**, *36* (1), 3−12.
(11) Ciesielski, T. M.; Pastukhov, M. V.; Szefer, P.; Jenssen, B. M. Bioaccumulation of mercury in the pelagic food chain of the Lake Baikal. *Chemosphere* **2010**, *78* (11), 1378−1384.
(12) Hammerschmidt, C. R.; Finiguerra, M.; Weller, R. L.; Fitzgerald, W. F. Methylmercury accumulation in plankton on the continental margin of the Northwest Atlantic Ocean. *Environ. Sci. Technol.* **2013**, *47* (8), 3671−3677.
(13) van der Velden, S.; Dempson, J.B.; Evans, M.S.; Muir, D.C.G.; Power, M. Basal mercury concentrations and biomagnification rates in freshwater and marine food webs: Effects on Arctic charr (*Salvelinus alpinus*) from eastern Canada. *Sci. Total Environ.* **2013**, *444*, 531−542.
(14) Gosnell, K. J.; Balcom, P. H.; Tobias, C. R.; Gilhooly, W. P.; Mason, R. P. Spatial and temporal trophic transfer dynamics of mercury and methylmercury into zooplankton and phytoplankton of Long Island Sound. *Limnol. Oceanogr.* **2017**, *62* (3), 1122−1138.
(15) Cardoso, P. G.; Pereira, E.; Duarte, A. C.; Azeiteiro, U. M. Temporal characterization of mercury accumulation at different trophic levels and implications for metal biomagnification along a coastal food web. *Mar. Pollut. Bull.* **2014**, *87* (1), 39−47.
(16) Ward, B. A.; Dutkiewicz, S.; Follows, M. J. Modelling spatial and temporal patterns in size-structured marine plankton communities: top−down and bottom−up controls. *J. Plankton Res.* **2014**, *36* (1), 31−47.
(17) Barton, A. D.; Dutkiewicz, S.; Flierl, G.; Bragg, J.; Follows, M. J. Patterns of diversity in marine phytoplankton. *Science* **2010**, *327* (5972), 1509−1511.
(18) Prowe, A. F.; Pahlow, M.; Dutkiewicz, S.; Oschlies, A. Small diversity effects on ocean primary production under environmental change in a diversity-resolving ocean ecosystem model. *Biogeosciences Discussions* **2013**, *10* (7), 12571−12591.
(19) Clayton, S.; Nagai, T.; Follows, M. J. Fine scale phytoplankton community structure across the Kuroshio Front. *J. Plankton Res.* **2014**, *34* (4), 1017−1030.
(20) Chen, C. Y.; Amirbahman, A.; Fisher, N. S.; Harding, G. C.; Lamborg, C. H.; Nacci, D.; Taylor, D. L. Methylmercury in marine ecosystems: spatial patterns and processes of production, bioaccumulation, and biomagnification. *Ecohealth* **2008**, *5* (4), 399−408.
(21) Ferriss, B. E.; Essington, T. E. Does trophic structure dictate mercury concentrations in top predators? A comparative analysis of pelagic food webs in the Pacific Ocean. *Ecol. Modell.* **2014**, *278*, 18−28.
(22) Booth, S.; Zeller, D. Mercury, food webs and marine mammals: implications of diet and climate change for human health. *Environ. Health Perspect.* **2005**, *113* (5), 521−526.
(23) Zeller, D.; Reinert, J. Modelling spatial closures and fishing effort restrictions in the Faroe Islands marine ecosystem. *Ecol. Modell.* **2004**, *172* (2), 403−420.
(24) Alava, J. J.; Cisneros-Montemayor, A. M.; Sumaila, U. R.; Cheung, W. W. L. Projected amplification of food web bioaccumulation of MeHg and PCBs under climate change in the Northeastern Pacific. *Sci. Rep.* **2018**, *8* (1), 13460.
(25) Zhang, Y.; Soerensen, A. L.; Schartup, A. T.; Sunderland, E. M. A global model for methylmercury formation and uptake at the base of marine food webs. *Global Biogeochem. Cycles* **2020**, 6348 DOI: 10.1029/2019GB006348.
(26) Zakem, E. J.; Alhaj, A.; Church, M. J.; Dijken, G. L. V.; Dutkiewicz, S.; Foster, S. Q.; Fulweiler, R. W.; Mills, M. M.; Follows, M. J. Ecological control of nitrite in the upper ocean. *Nat. Commun.* **2018**, *9* (1), 1206.
(27) Marshall, J.; Adcroft, A.; Hill, C.; Perelman, L. T.; Heisey, C. A finite-volume, incompressible Navier Stokes model for studies of the ocean on parallel computers. *Journal of Geophysical Research* **1997**, *102*, 5753−5766.
(28) Sokolov, A. I. *Phys. Solid State* **2005**, *47*, 2144.
(29) Large, W. G.; McWilliams, J. C.; Doney, S. C. Oceanic vertical mixing: A review and a model with a nonlocal boundary layer parameterization. *Rev. Geophys.* **1994**, *32* (4), 363−403.
(30) Gent, P. R.; Mcwilliams, J. C. Isopycnal mixing in ocean circulation models. *Journal of Physical Oceanography* **1990**, *20* (1), 150−155.
(31) Tilman, D. Resource competition between planktonic algae: An experimental and theoretical approach. *Ecology* **1977**, *58*, 338−348.
(32) Hansell, D. A.; Carlson, C. A.; Repeta, D. J.; Schlitzer, R. Dissolved organic matter in the ocean: A controversy stimulates new insights. *Oceanography* **2009**, *22* (4), 202−211.
(33) Taniguchi, D. A. A.; Franks, P. J. S.; Poulin, F. J. Planktonic biomass size spectra: an emergent property of size-dependent physiological rates, food web dynamics, and nutrient regimes. *Mar. Ecol.: Prog. Ser.* **2014**, *514*, 13−33.
(34) Zhang, Y.; Jacob, D. J.; Dutkiewicz, S.; Amos, H. M.; Long, M. S.; Sunderland, E. M. Biogeochemical drivers of the fate of riverine mercury discharged to the global and Arctic oceans. *Global Biogeochemical Cycles* **2015**, *29* (6), 854−864.
(35) Dutkiewicz, S.; Scott, J. R.; Follows, M. J. Winners and losers: Ecological and biogeochemical changes in a warming ocean. *Global Biogeochemical Cycles* **2013**, *27* (2), 463−477.
(36) Horowitz, H. M.; Jacob, D. J.; Zhang, Y.; Dibble, T. S.; Slemr, F.; Amos, H. M.; Schmidt, J. A.; Corbitt, E. S.; Marais, E. A.; Sunderland, E. M. A new mechanism for atmospheric mercury redox chemistry: implications for the global mercury budget. *Atmos. Chem. Phys.* **2017**, *17* (10), 6353−6371.
(37) Gregg, W. W.; Ginoux, P.; Schopf, P. S.; Casey, N. W. Phytoplankton and iron: validation of a global three-dimensional ocean biogeochemical model. *Deep Sea Res., Part II* **2003**, *50* (22), 3143−3169.
(38) Alvain, S.; Moulin, C.; Dandonneau, Y.; Loisel, H. Seasonal distribution and succession of dominant phytoplankton groups in the global ocean: A satellite view. *Global Biogeochemical Cycles* **2008**, *22* (3), 3154.
(39) Moriarty, R.; Obrien, T. D. Distribution of mesozooplankton biomass in the global ocean. *Earth System Science Data* **2013**, *5* (1), 45−55.
(40) Buitenhuis, E. T.; Li, W. K. W.; Vaulot, D.; Lomas, M. W.; Landry, M. R.; Partensky, F.; Karl, D. M.; Ulloa, O.; Campbell, L.; Jacquet, S.; Lantoine, F.; Chavez, F.; Macias, D.; Gosselin, M.; McManus, G. B. Picophytoplankton biomass distribution in the global ocean. *Earth System Science Data* **2012**, *4*, 37−46.
(41) Leblanc, K.; Aristegui, J.; Armand, L.; Assmy, P.; Beker, B.; Bode, A.; Breton, E.; Cornet, V.; Gibson, J.; Gosselin, M.-P.; Kopczynska, E.; Marshall, H.; Peloquin, J.; Piontkovski, S.; Poulton, A. J.; Queguiner, B.; Schiebel, R.; Shipe, R.; Stefels, J.; van Leeuwe, M. A.; Varela, M.; Widdicombe, C.; Yallop, M. A global diatom database -

abundance, biovolume and biomass in the world ocean. *Earth System Science Data* **2012**, *4* (1), 149−165.
(42) Buitenhuis, E. T.; Li, W. K. W.; Lomas, M. W.; Karl, D. M.; Landry, M. R.; Jacquet, S. Picoheterotroph (Bacteria and Archaea) biomass distribution in the global ocean. *Earth System Science Data* **2012**, *4* (1), 101−106.
(43) Ward, B. A.; Dutkiewicz, S.; Jahn, O.; Follows, M. J. A size-structured food-web model for the global ocean. *Limnol. Oceanogr.* **2012**, *57* (6), 1877−1891.
(44) Dutkiewicz, S.; Follows, M. J.; Bragg, J. G. Modeling the coupling of ocean ecology and biogeochemistry. *Global Biogeochemical Cycles* **2009**, *23* (4), 3405.
(45) van Someren Greve, H.; Kiørboe, T.; Almeda, R. Bottom-up behaviourally mediated trophic cascades in plankton food webs. *Proc. R. Soc. London, Ser. B* **2019**, *286* (1896), 20181664.
(46) Westberry, T. K.; Behrenfeld, M. J.; Siegel, D. A.; Boss, E. Carbon-based primary productivity modeling with vertically resolved photoacclimation. *Global Biogeochemical Cycles* **2008**, *22* (2), 3078 DOI: 10.1029/2007GB003078.
(47) Fisher, N. S. Accumulation of metals by marine picoplankton. *Mar. Biol.* **1985**, *87* (2), 137−142.
(48) Gosnell, K. J.; Mason, R. P. Mercury and methylmercury incidence and bioaccumulation in plankton from the central Pacific Ocean. *Mar. Chem.* **2015**, *177*, 772−780.
(49) Lee, C. S.; Fisher, N. S. Methylmercury uptake by diverse marine phytoplankton. *Limnol. Oceanogr.* **2016**, *61* (5), 1626−1639.
(50) Kainz, M. J.; Mazumder, A. Effect of algal and bacterial diet on methyl mercury concentrations in zooplankton. *Environ. Sci. Technol.* **2005**, *39* (6), 1666−1672.
(51) Hirota, R.; Fukuda, Y.; Chiba, J.; Tajima, S.; Fujiki, M. Mercury content of copepods (*Crustacea*) collected from the Antarctic Sea. *Polar Research Repository* **1989**, *2*, 65−70.
(52) Todorova, S. G.; Driscoll, C. T.; Matthews, D. A.; Effler, S. W. Zooplankton community changes confound the ciodilution theory of methylmercury accumulation in a recovering mercury-contaminated lake. *Environ. Sci. Technol.* **2015**, *49* (7), 4066−4071.
(53) Kainz, M.; Lucotte, M.; Parrish, C. C. Methyl mercury in zooplankton - The role of size, habitat, and food quality. *Can. J. Fish. Aquat. Sci.* **2002**, *59* (10), 1606−1615.
(54) Oremland, R. S. Methanogenic activity in plankton samples and fish intestines A mechanism for in situ methanogenesis in oceanic surface waters. *Limnol. Oceanogr.* **1979**, *24* (6), 1136−1141.
(55) Hirota, R.; Fujiki, M.; Tajima, S. Mercury contents of zooplankton collected in the tropical Pacific Ocean. *Nippon Suisan Gakkaishi* **1979**, *45* (11), 1449−1451.
(56) Hammerschmidt, C. R.; Fitzgerald, W. F. Bioaccumulation and trophic transfer of methylmercury in Long Island Sound. *Arch. Environ. Contam. Toxicol.* **2006**, *51* (3), 416−424.
(57) Fox, A. L.; Trefry, J. H.; Trocine, R. P.; Dunton, K. H.; Lasorsa, B. K.; Konar, B.; Ashjian, C. J.; Cooper, L. W. Mercury biomagnification in food webs of the northeastern Chukchi Sea, Alaskan Arctic. *Deep Sea Res., Part II* **2017**, *144*, 63−77.
(58) Kehrig, H.A.; Palermo, E.F.A.; Seixas, T.G.; Branco, C.W.C.; Moreira, I.; Malm, O. Trophic transfer of methylmercury and trace elements by tropical estuarine seston and plankton. *Estuarine, Coastal Shelf Sci.* **2009**, *85* (1), 36−44.
(59) Foster, K. L.; Stern, G. A.; Pazerniuk, M. A.; Hickie, B.; Walkusz, W.; Wang, F.; Macdonald, R. W. Mercury biomagnification in marine zooplankton food webs in Hudson Bay. *Environ. Sci. Technol.* **2012**, *46* (23), 12952−12959.
(60) Menden-Deuer, S.; Lessard, E. J. Carbon to volume relationships for dinoflagellates, diatoms, and other protist plankton. *Limnol. Oceanogr.* **2000**, *45* (3), 569−579.
(61) Hansen, P. J.; BjØrnsen, P. K.; Hansen, B. W. Zooplankton grazing and growth: scaling within the 2−2,000-μm body size range. *Limnol. Oceanogr.* **2000**, *45* (8), 1891−1891.
(62) Schindler, J. E. Food quality and zooplankton nutrition. *J. Anim. Ecol.* **1971**, *40* (3), 589−595.

https://dx.doi.org/10.1021/acs.est.9b06075
Environ. Sci. Technol. 2020, 54, 5446−5455